# Synaptic NMDA receptors in developing mouse hippocampal neurones: functional properties and sensitivity to ifenprodil

Eilon D. Kirson and Yoel Yaari

*Department of Physiology, Hebrew University-Hadassah School of Medicine, Jerusalem 91120, Israel*

1. Whole-cell patch-clamp techniques were used to record pharmacologically isolated NMDA receptor-mediated EPSCs (NMDA EPSCs) from CA1 pyramidal cells (PCs) in hippocampal slices from 4-day-old to 36-week-old mice, in order to characterize developmental changes in functional properties and subunit composition of synaptic NMDA receptors.

2. During the first postnatal weeks the dendritic tree of CA1 PCs stained with biocytin increased both in size and in complexity. This was associated with an increase in amplitude of the focally evoked NMDA EPSCs recorded either in nominally $Mg^{2+}$-free or $Mg^{2+}$-containing saline. In adult PCs (>5 weeks old) EPSC amplitude was 4-fold larger than in very young (up to 2 weeks old) neurones.

3. The sensitivity of NMDA EPSCs to blockade by $Mg^{2+}$ did not change with age. In very young, intermediate and adult PCs the EPSC–voltage relation displayed an area of negative slope conductance at membrane potentials more negative than −30 mV. The apparent $K_d$ values of the NMDA receptors for $Mg^{2+}$ at 0 mV were 7·8 ± 6·4, 10·4 ± 14·1 and 6·5 ± 4·7 mM in very young, intermediate and adult neurones, respectively.

4. The decay of the NMDA EPSC in both young and adult neurones could be described by the sum of a fast and a slow exponential function. Both EPSC rise time and fast and slow decay time constants measured at −60 mV, decreased with age.

5. The decay of NMDA EPSCs in young *versus* adult PCs was differentially modulated by membrane voltage. In young PCs depolarization slowed both the fast and the slow EPSC components. In adult PCs depolarization slightly accelerated the initial EPSC decay, though the overall duration of the EPSC did not change. The rise time of the EPSCs was not affected by voltage at any age.

6. The subunit-selective NMDA receptor antagonist ifenprodil similarly blocked iontophoretic NMDA-induced currents and NMDA EPSCs. In both young and adult PCs, the concentration–response curves for this effect disclosed distinct low and high affinity binding sites for ifenprodil.

7. In young PCs, low and high affinity binding sites for ifenprodil were about equally expressed (57 *versus* 43%, respectively), whereas in adult PCs, synaptic NMDA receptors expressed a majority (78%) of low affinity binding sites for ifenprodil.

8. The long duration of NMDA EPSCs (and by implication, of $Ca^{2+}$ transfer through NMDA receptor channels) and its further prolongation by depolarization in young PCs are consistent with heightened NMDA-dependent neuronal plasticity early in development. The age-related changes in these properties may result from a developmental change in NMDA receptor subunit composition.

The *N*-methyl-D-aspartate (NMDA) subtype of glutamate receptors plays a major role in central synaptic transmission (e.g. Armstrong-James, Welker & Callahan, 1993), in various forms of neuronal plasticity (Bliss & Collingridge, 1993) and in excitotoxic brain damage (Diemer, Valente, Bruhn, Berg, Jorgensen & Johansen, 1993). Some properties of NMDA receptors appear to change throughout postnatal development. Thus, the decay kinetics of NMDA receptor-mediated excitatory postsynaptic currents (NMDA EPSCs) become faster with age (Hestrin, 1992; Carmignoto & Vicini, 1992). It has also been suggested that the sensitivity of NMDA receptors to blockade by $Mg^{2+}$ is absent or low in young neurones and increases with age (Bowe & Nadler, 1990; Kleckner & Dingledine, 1991), though, more recently,

contradictory results have been reported (Strecker, Jackson & Dudek, 1994). These developmental changes may underlie age-related differences in functional properties of synaptic NMDA receptors.

Native NMDA receptors are believed to be multimeric proteins (for review see Mori & Mishina, 1995). Five subunits of the NMDA receptor have been cloned, namely, NR1 and NR2A–D in the rat (Moriyoshi, Masayuki, Takahiro, Ryuichi, Mizuno & Nakanishi, 1991) and the homologous $\zeta 1$ and $\epsilon 1$–4 in the mouse (Kutsuwada *et al.* 1992), but it is not yet known which and how many subunits are assembled in a single receptor (Wafford, Bain, Le Bourdelles, Whiting & Kemp, 1993). Most probably different subunit compositions may occur naturally, since the four NR2 subunits are differentially expressed throughout the rodent brain. The expression profile of the different subunits throughout the brain changes with development (Mori & Mishina, 1995), suggesting a possible causal relation between changes in subunit composition and in functional properties of these receptors.

It has been shown that co-expression in host cells of the NR1/$\zeta 1$ subunit with any member of the NR2/$\epsilon$ family will form functional NMDA receptors (Mori & Mishina, 1995). However, the four heteromeric receptors differ in several macroscopic features, depending on the identity of the NR2 subunit. Firstly, the sensitivity to $Mg^{2+}$ block ranks in the following order: NR1–NR2A $\approx$ NR1–NR2B > NR1–NR2C $\approx$ NR1–NR2D (Monyer *et al.* 1992). Secondly, the offset kinetics of L-glutamate-induced currents mediated by the NR1–NR2A heteromer are faster (of the order of tens of milliseconds) than those mediated by the NR1–NR2B and the NR1–NR2C heteromers (of the order of hundreds of milliseconds) and the NR1–NR2D heteromer (of the order of seconds; Monyer *et al.* 1992; Monyer, Burnashev, Laurie, Sakmann & Seeburg, 1994). This is most probably inversely related to the affinity of these heteromers for L-glutamate, which is highest for NR1–NR2D and lowest for NR1–NR2A (Mori & Mishina, 1995). Thirdly, the NMDA antagonist ifenprodil (Legendre & Westbrook, 1991) differentiates between different heteromers (Williams, Russell, Shen & Molinoff, 1993; Williams, 1993, 1995). The NR1–NR2A combination has a low affinity for ifenprodil, whereas the NR1–NR2B combination has a 400-fold higher affinity for the antagonist. Additional pharmacological differences between the four heteromers have been described (Mori & Mishina, 1995).

The distinct features of the four different recombinant heteromeric NMDA receptors may be used to infer the subunit composition of native synaptic NMDA receptors and its modification through development. Using this approach, we have characterized the $Mg^{2+}$ sensitivity, the kinetic properties, and the ifenprodil block of NMDA EPSCs in young *versus* adult hippocampal pyramidal neurones *in situ*. Our data are consistent with the hypothesis that glutamatergic synapses in young mouse hippocampal CA1 pyramidal cells (PCs) express NR1–NR2A and NR1–NR2B subunit combinations in equal amounts and that the relative expression of NR1–NR2A becomes predominant in the adult.

## METHODS

### Slice preparation

Experiments were performed on thin hippocampal slices obtained from 4-day-old to 36-week-old Sabra mice. Methods for preparation of thin slices were similar to those described previously (Edwards, Konnerth, Sakmann & Takahashi, 1989; Perouansky, Baranov, Salman & Yaari, 1995). Briefly, mice were anaesthetized with ether (5 ml vaporized in a closed chamber) and decapitated with a guillotine. The brain was removed and immediately immersed in an ice-cold oxygenated (95% $O_2$–5% $CO_2$) dissection saline. The caudal two-thirds of one hemisphere (containing one hippocampus) was glued to the stage of a vibratome (FTB). Transverse slices, 150–180 $\mu$m thick, were cut from the region of the hemisphere containing the anterior hippocampus. The hippocampal portion was dissected out of each slice and transferred to an incubation chamber containing oxygenated incubation saline at 34 °C. After an incubation period of at least 1 h, slices were transferred, one at a time, to a recording chamber where they were continuously perfused (2·5 ml $min^{-1}$) with oxygenated experimental saline at room temperature (21–24 °C).

### Solutions

The dissection saline consisted of (mM): NaCl, 125; KCl, 2·5; $NaHCO_3$, 26·7; Hepes, 13; $NaH_2PO_4$, 1·25; glucose, 6·3; $CaCl_2$, 0·5; and $MgSO_4$, 4; with a pH of 7·3. The incubation saline was identical except for $NaHCO_3$, which was 22·5 mM in order to maintain pH 7·3 at 34 °C. The standard experimental saline consisted of (mM): NaCl, 125; KCl, 2·5; $NaHCO_3$, 26·7; Hepes, 13; glucose, 12·5; $CaCl_2$, 2·5; $MgCl_2$, 1; with a pH of 7·3; osmolarity was 300 mosmol $l^{-1}$. In $Mg^{2+}$-free saline $MgCl_2$ was omitted. All salines also contained bicuculline methiodide (10 $\mu$M) to block GABA-mediated chloride currents and glycine (5 $\mu$M) to saturate the glycine-binding sites in NMDA receptors. In iontophoresis experiments 0·5 $\mu$M tetrodotoxin was added to the saline in order to block all synaptic transmission. The intracellular (pipette) solution in all experiments consisted of (mM): CsF, 130; NaCl, 10; EGTA, 10; Hepes, 10; $MgCl_2$, 2; $CaCl_2$, 1; at a pH of 7·2 and osmolarity of 280 mosmol $l^{-1}$. In some experiments biocytin (0·7%) was included in the intracellular solution.

All drugs were purchased from Sigma with the exception of 6-cyano-7-nitro-quinoxaline-2,3-dione (CNQX) which was from Tocris Neuramin and biocytin from Molecular Probes.

### Whole-cell recordings

Cells in the CA1 field were visualized at ×400 magnification with Nomarski optics using an upright Zeiss standard 18 microscope. Cells were identified as PCs by their position in the pyramidal layer, the pyramidal shape of their somata and their prominent apical dendrite. Some cells ($n = 23$) were filled with biocytin for *post hoc* identification. In all but one case the labelled cells were typical PCs (see Fig. 1).

Recording pipettes were pulled from borosilicate glass on a vertical puller (List) and coated with at least one layer of Sylgard resin (Dow Corning). Pipette resistances were 3–10 MΩ when filled with CsF-based intracellular solution. After establishing the whole-cell recording configuration, series resistance was compensated for by setting the series resistance compensation control of the amplifier (List LM-EPC-7 or Axopatch 200A) to 60–90%. Series resistance

was monitored regularly throughout each experiment by measuring the current response to a 4 ms hyperpolarizing voltage step (5 mV). Experiments in which the series resistance exceeded 20 MΩ were discarded. Cleaning and/or stimulating pipettes were pulled from Boralex disposable micropipettes (Rochester Scientific) to a tip diameter of 6–10 μm and filled with saline. When necessary, these pipettes were first used to clear the surface of the cell somata from debris and then placed in the stratum radiatum for stimulation of afferent fibres. The distance from the pyramidal layer to the stimulation site was kept < 100 μm in order to stimulate mainly proximal apical dendritic synapses, thereby minimizing space-clamp errors and dendritic filtering (Spruston, Jaffe, Williams & Johnston, 1993).

Currents recorded were filtered on-line at 1–2 kHz, digitized at a sampling rate of 2–4 kHz and analysed off-line using a 486DX personal computer and commercial software (pCLAMP, Axon Instruments).

### Iontophoresis

A double-barrelled electrode was used for NMDA or α-amino-3-hydroxy-5-methylisoxazole-4-propionate (AMPA) iontophoresis. One barrel (~100 MΩ) contained 100 mM NMDA or 100 mM AMPA in 50 mM NaCl, and the other barrel (~20 MΩ) contained 150 mM NaCl. The tip of the electrode was placed about 100 μm apical to the soma of the patched cell. NMDA was ejected by passing 50 nA to 1 μA for 0·1–1 s. A retaining current of up to 10 nA was used to avoid leak of NMDA. At the beginning of each experiment, ejection and retaining currents were adjusted until the responses to stimuli delivered at 0·02 Hz were stable for at least 5 min.

### Pharmacological procedures

Ifenprodil (If) was bath applied after stable baseline recordings were obtained for at least 6 min. Maximal inhibition was seen 6–12 min after application and in some cases could be reversed by 12–40 min washout of the drug. When multiple doses were tested in single neurones, ifenprodil was washed out for 12–20 min before the next dose was applied. Typical recordings lasted 1–1·5 h allowing two to three doses to be tested.

The concentration–response curves for ifenprodil were either fitted with a one-site or a two-site binding scheme using the following functions:

$$\frac{I}{I_{max}} = \frac{EC_{50}}{[If] + EC_{50}} \quad \text{(one site)}, \qquad (1)$$

$$\frac{I}{I_{max}} = \frac{f_{high}EC_{50(high)}}{[If] + EC_{50(high)}} + \frac{f_{low}EC_{50(low)}}{[If] + EC_{50(low)}} \quad \text{(two sites)}. \qquad (2)$$

Where $I$ is the measured current, $I_{max}$ is the control current amplitude before adding ifenprodil, $f_{high}$ and $f_{low}$ are the fractions of the high and low affinity components of inhibition ($f_{high} + f_{low} = 1$), the $EC_{50}$ values are the corresponding $EC_{50}$ values for ifenprodil, and [If] is the concentration of ifenprodil tested.

### Cell staining

For staining putative PCs, recordings were made with biocytin-containing pipettes. Biocytin entered the cells by passive diffusion or was injected by holding the cell at depolarized potentials for several minutes. In a given slice only one cell was stained. Following the experiment the slices were fixed overnight in a 4% paraformaldehyde solution and incubated with avidin–biotin complex (Vectastain ABC Elite kit, Vector). The labelled cells were photographed at × 250 magnification.

### Data evaluation

The data were divided into two age groups: young (1–4 weeks old) and adult (> 5 weeks old) mice. For some measurements the young group was further divided into very young (1–2 weeks old) and intermediate (3–4 weeks old) subgroups.

The analysis of mean evoked EPSC values was performed on 20–50 and 5–10 consecutive traces in young and adult PCs, respectively. Rise times of NMDA EPSCs were measured as the time from 10 to 90% of the peak current. Decay of NMDA EPSCs were fitted with the sum of two exponential functions:

$$y = A_f \exp(-t/\tau_f) + A_s \exp(-t/\tau_s), \qquad (3)$$

where $A$ is the current amplitude, $t$ is time, $\tau$ is the decay time constant and the subscripts 'f' and 's' denote fast and slow components, respectively.

Current–voltage ($I$–$V$) relations of NMDA EPSC values were fitted with a theoretical function describing the $I$–$V$ relation of these currents (Perouansky & Yaari, 1993):

$$I = \frac{a g_{max}(V - V_r)}{a + [Mg^{2+}]_o \exp(-bV)}, \qquad (4)$$

where $I$ is the maximal current at a given holding potential $V$, $g_{max}$ is the maximal conductance, $V_r$ is the reversal potential of the EPSC, $[Mg^{2+}]_o$ is the extracellular $Mg^{2+}$ concentration and $a$ and $b$ are constant parameters. The derivation of this function is based on the assumption that the $K_d$ for $Mg^{2+}$ binding is exponentially related to membrane potential (Ascher & Nowak, 1988), that is:

$$K_d = a\exp(-bV). \qquad (5)$$

In order to calculate the apparent $K_d$ for the $I$–$V$ relations of recombinant heteromeric NMDA receptors (Monyer *et al.* 1994), the published curves were scanned, digitized and fitted with the above functions.

### Statistical analysis

Data are presented as means ± standard deviation (S.D.) or standard error of the mean (S.E.M.) as indicated. Large samples of data were tested for normal distribution using the $\chi^2$ test. When the distribution deviated significantly from normal or the sample size was less than twenty, significant differences between pairs of samples were tested with either a Mann–Whitney $U$ test or a Wilcoxon matched pairs test. Otherwise, Student's $t$ test was used. A significance level of $\alpha = 0{\cdot}05$ and $P < 0{\cdot}05$ was applied to all tests. Pearson linear correlation was employed in order to find correlations between pairs of variables. Fitting procedures used the Levenberg–Marquardt non-linear least-squares algorithm to seek parameter values that minimize the sum of the squared differences between the observed and predicted values of the dependent variables.

## RESULTS

### Developmental changes in PC morphology

In the rat hippocampus, CA1 PCs continue to grow post-natally. Growth is expressed in elongation, proliferation and ramification of both basilar and apical dendrites (Pokorny & Yamamoto, 1981). Though we did not study these aspects quantitatively, a similar process of dendritic growth and branching was evident in mouse PCs ($n = 22$). The biocytin-

stained PCs shown in Fig. 1 illustrate the morphology of the PCs in the three age groups investigated in this study.

**Developmental increase in amplitude of NMDA EPSCs**

It has been previously shown that native glutamatergic EPSCs in mouse CA1 PCs comprise a fast, non-NMDA receptor-mediated component in addition to the slow component mediated by NMDA receptors (Perouansky *et al.* 1995). In the present experiments the NMDA EPSC was isolated by bath application of the non-NMDA receptor antagonist CNQX (5 $\mu$M), which entirely suppressed the non-NMDA EPSC (Perouansky *et al.* 1995). The following data were obtained by recording pharmacologically isolated NMDA and non-NMDA EPSCs in a total of 180 PCs.

For comparing the size of NMDA EPSCs from different age groups, the EPSCs were recorded at the same membrane potential (−60 mV) in $Mg^{2+}$-free and/or in $Mg^{2+}$-containing saline (Fig. 2*A*). In each neurone, stimulus intensity was increased until a maximal synaptic response was obtained. In either saline, the amplitude of NMDA EPSCs increased significantly with age, being 4-fold larger in adult than in very young PCs (Fig. 2*B*, Table 1). The fraction of EPSC blocked by $Mg^{2+}$ at −60 mV remained similar at all ages (Fig. 2*C*), suggesting that the affinity of synaptic NMDA receptors to $Mg^{2+}$ does not change significantly after the fifth postnatal day.

**$Mg^{2+}$ sensitivity of NMDA EPSCs in young *versus* adult PCs**

The latter notion was further tested by comparing the *I–V* relations of NMDA EPSCs evoked in $Mg^{2+}$-containing saline in very young (1–2 weeks old), intermediate (3–4 weeks old) and adult (>5 weeks old) PCs ($n = 33$). The *I–V* curves were constructed from NMDA EPSC values recorded at holding potentials between −90 and +30 mV. In all three cases, the

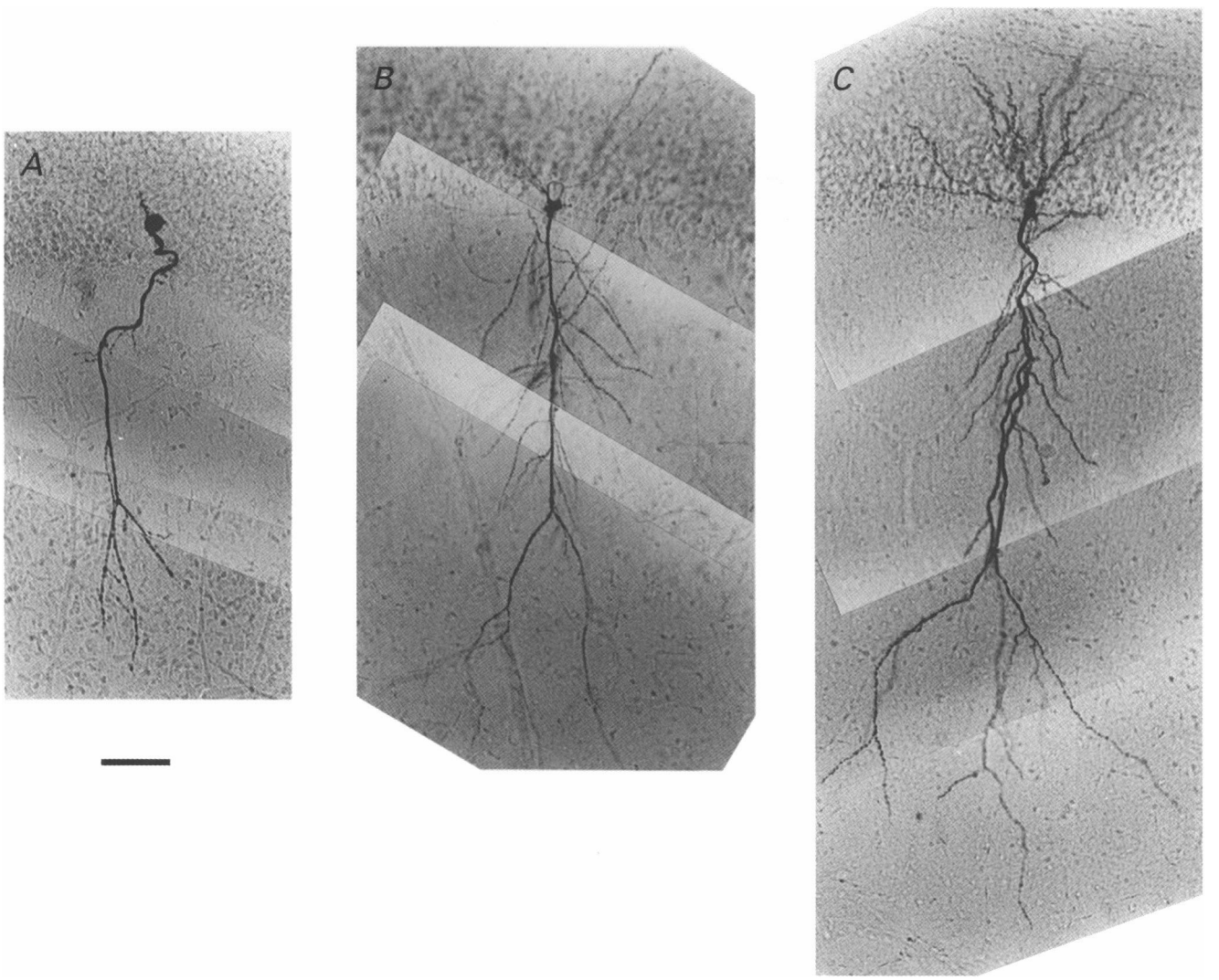


**Figure 1. Developmental increase in size and complexity of PC dendritic trees**

Photomicrographs of biocytin-stained PCs in slices of different ages. *A*, 5-day-old PC; *B*, 27-day-old PC; *C*, 70-day-old PC. Scale bar represents 50 $\mu$m for all panels.

$I$–$V$ curves were J shaped and had an area of negative slope conductance at holding potentials more negative than −30 mV (Fig. 3). For statistical comparison the $I$–$V$ curves in each group were normalized and averaged. No significant differences between the different age groups were found at any given holding potential ($P > 0{\cdot}05$, Mann–Whitney $U$ test). Conductance–voltage relations were calculated from the $I$–$V$ curves and fitted with a simple Boltzmann equation (Fig. 3, insets). No differences in either voltage sensitivity or slope of the EPSC conductance were seen between the different age groups.

The negative slope conductance in the $I$–$V$ relation of NMDA EPSCs results from the voltage-dependent block of open NMDA receptor channels by extracellular $Mg^{2+}$ (Nowak, Bregestovski, Ascher, Herbert & Prochiantz, 1984). The apparent dissociation constant ($K_d$) for $Mg^{2+}$ binding at each membrane potential can be deduced from the $I$–$V$ relation (Perouansky & Yaari, 1993; see Methods). At 0 mV the apparent $K_d$ for $Mg^{2+}$ was 7·8 ± 6·4, 10·4 ± 14·1 and 6·5 ± 4·7 mM in slices from very young, intermediate and adult mice, respectively (means ± S.D.; differences not significant). Changing to $Mg^{2+}$-free saline markedly shifted the region of

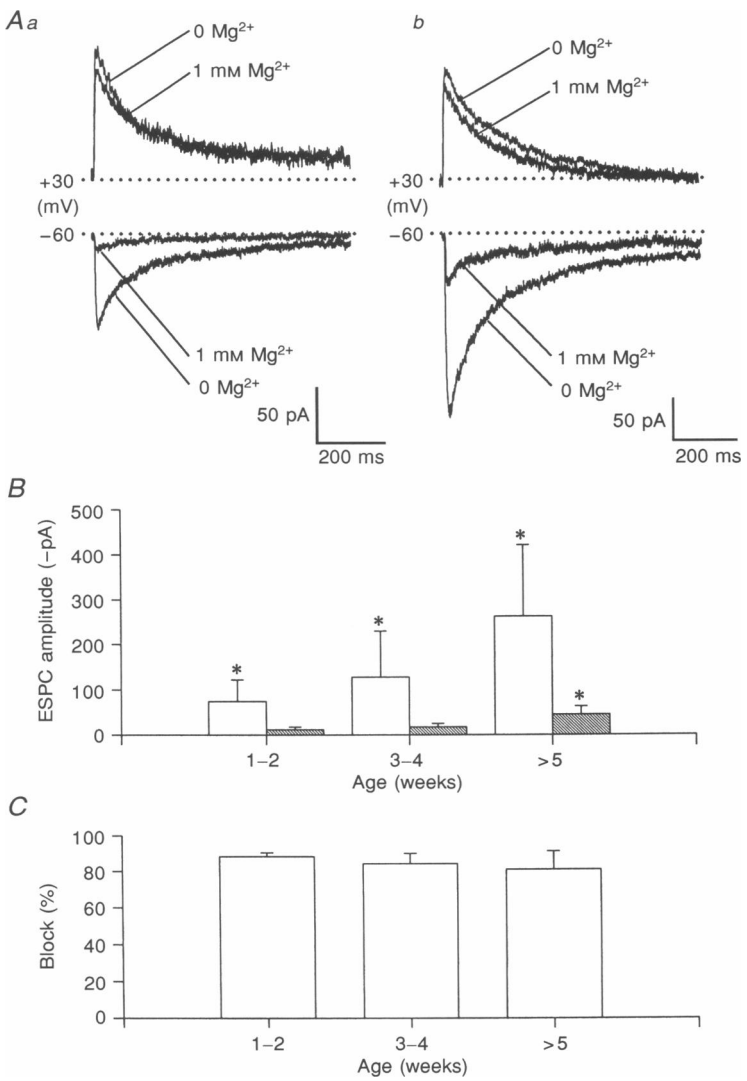


**Figure 2. Developmental increase in size of NMDA EPSC values in PCs**

Recordings were made in the presence of 5 μM CNQX at two holding potentials, as indicated. *A*, representative NMDA EPSCs in slices from a young (22 days old; *A a*) and an adult mouse (17 weeks old; *A b*). At −60 mV, the EPSCs evoked in nominally $Mg^{2+}$-free saline were reduced to 18·5% (*A a*) and to 27·4% (*A b*) of the control 5 min after exchange to $Mg^{2+}$-containing saline. At +30 mV, the $Mg^{2+}$ block of the EPSCs was small. *B*, mean NMDA EPSC amplitudes evoked in $Mg^{2+}$-containing (▨) and $Mg^{2+}$-free saline (□) in the three age groups (means ± S.D.). The EPSCs were elicited by near-maximal stimulation intensity. * denote significant differences from both other age groups ($P < 0{\cdot}05$, Student's $t$ test). *C*, the mean block of NMDA EPSCs obtained by adding 1 mM $Mg^{2+}$ to the nominally $Mg^{2+}$-free saline in the three age groups (means ± S.D.). The differences in $Mg^{2+}$ block between the three groups were not significant ($P > 0{\cdot}05$, Mann–Whitney $U$ test).

negative slope conductance to more hyperpolarized holding potentials at all ages tested (data not shown).

The NMDA EPSCs reversed at a membrane potential of 4·6 ± 4·1 ($n = 14$), 2·1 ± 3·7 ($n = 24$) and 3·8 ± 3·8 mV ($n = 18$) in very young, intermediate and adult neurones, respectively (means ± S.D.; differences not significant). These values are similar to those previously found in juvenile rat hippocampal neurones (Keller, Konnerth & Yaari, 1991; Perouansky & Yaari, 1993) and suggest that the ion selectivity of NMDA receptor channels does not change appreciably during postnatal development.

### Evaluation of space-clamp errors

Even though we stimulated afferent fibres near (< 100 μm) the PC soma, it is possible, especially in adult PCs, that the complex dendritic geometry will impose imperfect space-clamp conditions, thereby distorting the waveform of the EPSCs. We evaluated this problem in two complementary ways (Spruston *et al.* 1993). First, we looked at whether holding the neurone at the EPSC reversal potential would affect subsequent EPSC decay. The experimental protocol and representative results are illustrated in Fig. 4*A*. Synaptic stimulation was delivered while the membrane potential was held at the EPSC reversal potential (~0 mV), so that no net current was flowing through the synaptic conductance. In sequential repetitions of this protocol, the membrane potential was stepped to −60 mV at increasing intervals (200, 400, 600 and 800 ms) after stimulation. Responses to the same voltage commands without synaptic stimulation were subtracted from the EPSC recordings. The decay time of the residual EPSCs appearing at −60 mV reflect the deactivation time course of the synaptic conductance (Pearce, 1993). These decay times matched exactly the decay time of the EPSC evoked at −60 mV (Fig. 4*A*), indicating that the latter is not distorted by dendritic filtering. Similar results were obtained in five adult CA1 PCs.

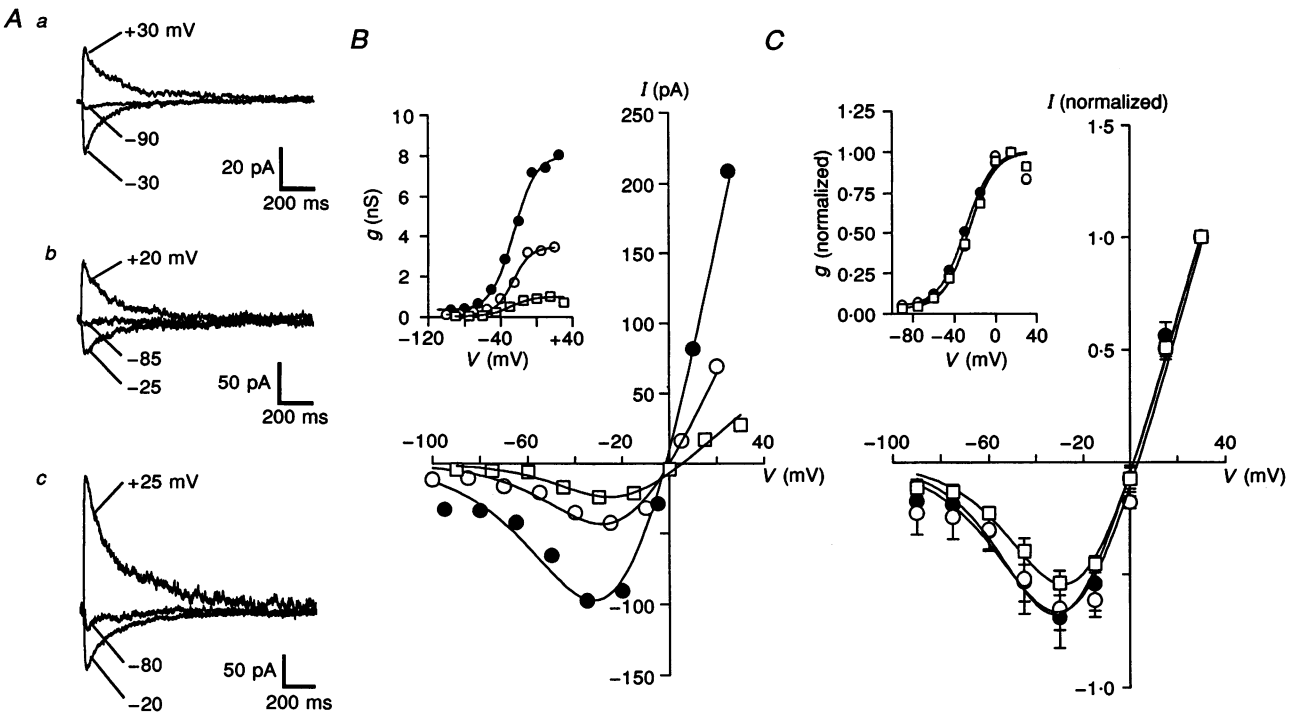


**Figure 3. Voltage dependence of NMDA EPSCs in young *versus* adult PCs in $Mg^{2+}$-containing saline**

*A*, exemplary EPSCs recorded at the indicated holding potentials in slices from a very young (8 days old; *A a*), an intermediate (21 days old; *A b*) and an adult mouse (18 weeks old; *A c*). *B*, superimposed *I–V* relations of the EPSCs from the three experiments illustrated in *A* (*a*, □; *b*, ○ and *c*, ●). Maximal inward current was evoked at about −30 mV in all cases. Note the similar voltage range of negative slope conductance in all relations. The conductance–voltage relations are shown in the inset. Both slope and voltage sensitivity of these curves were similar in the very young (□), intermediate (○) and the adult neurones (●). *C*, mean *I–V* relations of NMDA EPSCs in $Mg^{2+}$-containing saline in PCs from very young (1–2 weeks old; $n = 12$; □), intermediate (3–4 weeks old; $n = 11$; ○) and adult mice (> 5 weeks old; $n = 10$; ●). The EPSC amplitudes were normalized to the currents obtained in each cell at +30 mV (where $Mg^{2+}$ block is minimal). Bars indicate S.E.M. The normalized EPSC values in each group were not significantly different at any given potential ($P > 0{\cdot}05$, Mann–Whitney *U* test). The mean conductance–voltage relations are shown in the inset. The continuous lines in the *I–V* relations were obtained by fitting eqn (4) through the data points (see Methods).

Second, we tested for correlations between EPSC rise times and decay time constants (Fig. 4*B*) and between EPSC amplitudes and time constants (Fig. 4*C*). If the EPSC decay kinetics are affected by dendritic filtering, then positive correlations between these variables are expected (Spruston *et al.* 1993). However, no such correlations were found (Pearson linear correlation).

### Developmental changes in NMDA EPSC rise time and decay

Comparison of the NMDA EPSC kinetics in different age groups were made by recording the EPSCs at the same membrane potential (−60 mV) in $Mg^{2+}$-free saline. The NMDA EPSCs at all ages exhibited a slow biphasic decay, which was best fitted with a double-exponential function

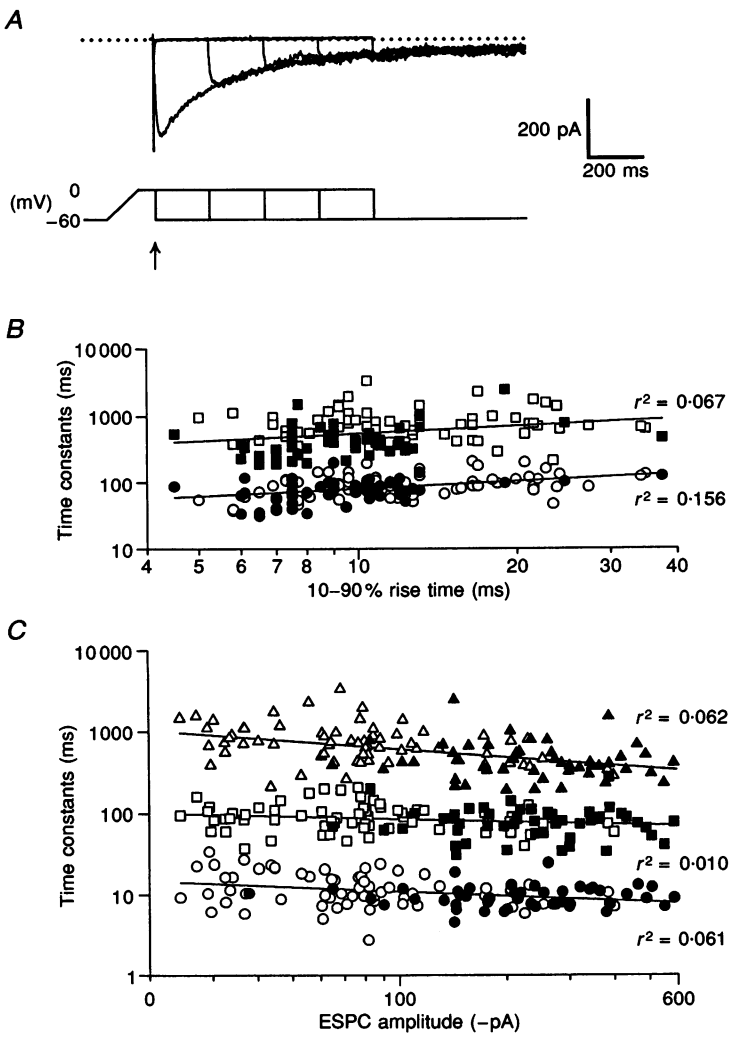


**Figure 4. Evaluation of the efficacy of space clamping NMDA EPSCs in adult PCs**

*A*, test for the true decay of the synaptic conductance in a 17-week-old PC. The lower traces describe the waveform of the voltage steps. Each trial began by stepping the membrane potential from −60 to 0 mV (the approximate EPSC reversal potential), after which the EPSC was evoked at the time indicated by the arrow. In five consecutive trials, the membrane potential was maintained at 0 mV for increasingly longer durations after stimulation (0, 200, 400, 600 and 800 ms) and was then stepped back to −60 mV. Similar trials were repeated also without synaptic stimulation. The upper traces depict the EPSCs evoked in each trial after subtraction of the corresponding responses obtained without synaptic stimulation. No synaptic current was seen at 0 mV. Stepping back to −60 mV induced a current which decayed along a similar time course in all trials. This indicates that the EPSC decay is due solely to decay of the synaptic conductance. *B*, plots of the fast ($\tau_f$, ○ and ●) and the slow decay time constants ($\tau_s$, ■ and □) *versus* the rise times of NMDA EPSCs in 66 young (open symbols) and 49 adult PCs (closed symbols). No correlation was found between these variables (Pearson linear correlation; $r^2$ values are shown by their corresponding plots). *C*, plots of the rise times (○ and ●) and the fast ($\tau_f$, ■ and □) and slow decay time constants ($\tau_s$, △ and ▲) of NMDA EPSCs *versus* their amplitudes in the same neurones. No correlation was found between these variables (Pearson linear correlation; $r^2$ values are shown by their corresponding plots).

(Fig. 5A). The fast ($\tau_f$) and slow ($\tau_s$) decay time constants varied considerably, with a skewed distribution that was significantly different from normal ($P < 0{\cdot}05$, $\chi^2$ test). Both decay time constants decreased significantly with age; $\tau_f$ decreased by 12·5% and $\tau_s$ by 42·6% from 1- to 2-week-old to adult PCs (Fig. 5B, Table 1). The relative contribution of the two components of decay remained similar at all ages, The fast decay component $A_f$ constituting between 56 and 61% of the EPSC (Fig. 5C, Table 1).

The 10–90% rise times of the EPSCs became shorter with age (Fig. 6A). The EPSC rise times in adult PCs were significantly shorter than in young PCs, though no difference was found between the 1- to 2-week-old and 3- to 4-week-old PCs (Fig. 6B, Table 1).

## Developmental switch in the voltage dependence of NMDA EPSC decay

Previous studies in some young rat brain neurones (Konnerth, Keller, Ballanyi & Yaari, 1990; Hestrin, 1992), though not in others (Perouansky & Yaari, 1993; Sah, Hestrin & Nicoll, 1990), have shown that the decay of NMDA EPSCs is voltage dependent. Even in the absence of extracellular $Mg^{2+}$, depolarization prolonged the EPSC decay. We examined whether this property is manifested in mouse CA1 PCs and whether it is developmentally regulated.

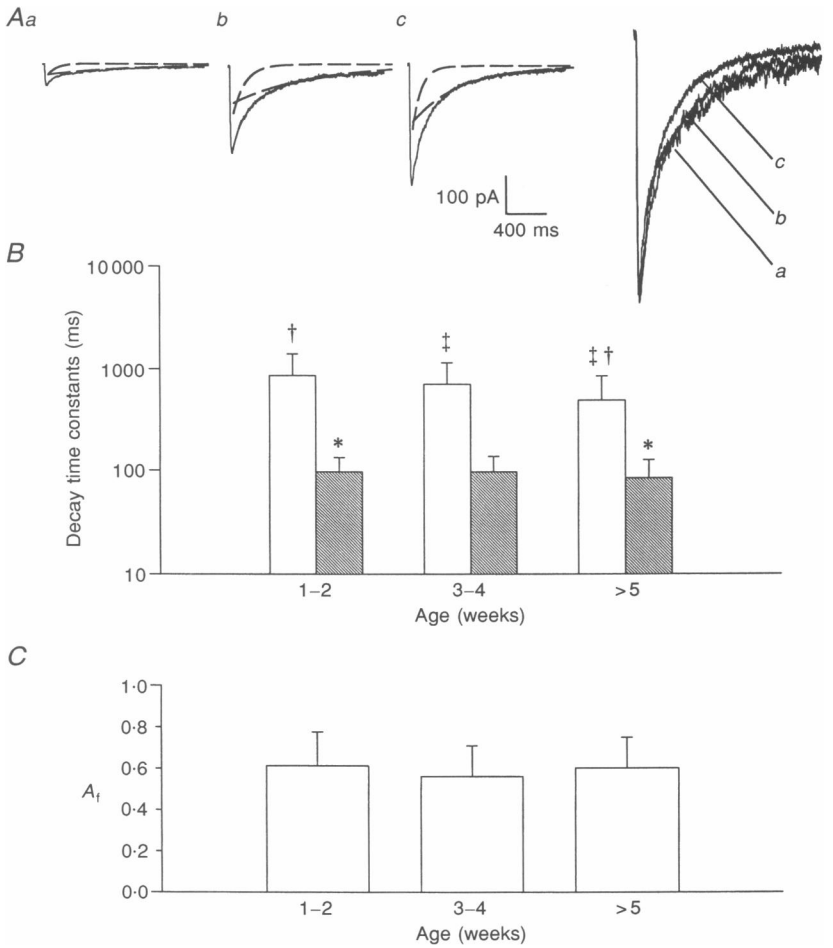


**Figure 5. The decay kinetics of isolated NMDA EPSCs become faster with age**

Comparisons were made between NMDA EPSCs evoked in $Mg^{2+}$-free saline at −60 mV. *A*, representative EPSCs in a 12-day-old (*A a*), 19-day-old (*A b*) and 16-week-old PC (*A c*). In all cases, the time course of EPSC decay was best fitted by the sum of two exponential functions (eqn (3) in Methods). The two functions (dashed lines) are shown superimposed on each of the EPSCs. Their respective fast ($\tau_f$) and slow ($\tau_s$) decay time constants are 81·6 and 853·8 (*A a*), 124·8 and 789·2 (*A b*) and 87·1 and 472·0 ms (*A c*). The same traces are normalized and superimposed on the right. *B*, the fast ($\tau_f$, ▨) and slow decay time constants ($\tau_s$, □) (means ± S.D.) of NMDA EPSCs recorded from 1- to 2-week-old ($n = 43$), 3- to 4-week-old ($n = 26$) and >5-week-old PCs ($n = 52$). Columns labelled with the same symbols are significantly different from each other ($P < 0{\cdot}05$, Mann–Whitney *U* test). Note semilogarithmic scale. *C*, the partial contribution of the fast decay component ($A_f$) to EPSC amplitude in the above age groups (means ± S.D.). No significant differences were found between groups ($P > 0{\cdot}05$, Student's *t* test).

Exemplary NMDA EPSCs from a young PC are shown in Fig. 7*A*. The EPSC recorded at +30 mV was slower than that evoked at −60 mV (panel *A a*), as readily seen after superimposing the scaled traces (panel *A b*). Fitting the two decay times with the double-exponential functions indicated that both $\tau_f$ and $\tau_s$ were longer at +30 mV than at −60 mV. The relations of $\tau_f$ and $\tau_s$ of NMDA EPSCs *versus* membrane potential in 1- to 4-week-old PCs ($n = 30$) are shown in Fig. 7*B*. A significant positive correlation was found between each EPSC component and membrane potential (Pearson linear correlation), with an e-fold increase of $\tau_f$ and $\tau_s$ every 343 and 121 mV, respectively. These changes in $\tau_f$ and $\tau_s$ were not accompanied by significant changes in the relative size of each decay time component.

In contrast, the overall decay time of NMDA EPSCs in adult PCs did not change with depolarization (Fig. 7*C*). However, the fast decay time component appeared to be slightly accelerated by depolarization. The relations of $\tau_f$ and $\tau_s$ of NMDA EPSCs *versus* membrane potential in these neurones ($n = 10$) are shown in Fig. 7*D*. A significant negative correlation was found only between $\tau_f$ and membrane potential (Pearson linear correlation), with an e-fold decrease per 167 mV. The relative size of each EPSC decay time component also was not affected by membrane potential also in adult PCs.

The rise times of NMDA EPSCs evoked at membrane potentials between −90 and +30 mV were insensitive to membrane potential in both young ($n = 17$) and adult ($n = 8$) CA1 PCs (Fig. 8).

### Ifenprodil block of NMDA EPSCs in young *versus* adult PCs

In the whole brain a developmental increase in expression of the NR2A subunit is associated with an increase in the fraction of low affinity ifenprodil binding to native NMDA receptors (Williams *et al.* 1993). We reasoned that if such changes occur in hippocampal PCs, then the efficacy of ifenprodil in blocking NMDA EPSCs would decrease with age.

We compared the inhibitory effect of ifenprodil on NMDA EPSCs in young *versus* adult CA1 PCs. In each case, ifenprodil blocked NMDA EPSCs in a concentration-dependent manner over a wide range of concentrations (0·01–100 $\mu$M). However, NMDA EPSCs in young PCs were much more sensitive to the drug than in adult PCs. Figure 9 provides the cumulative concentration–response relation of ifenprodil in twenty-three young and thirty adult PCs. Both relations were clearly biphasic and fitted a two binding-site model of block (see Methods). In young neurones, 43% of the binding sites showed a high affinity for ifenprodil ($EC_{50} = 0{\cdot}010$ $\mu$M), whereas 57% showed a low affinity for the drug ($EC_{50} = 6{\cdot}6$ $\mu$M). In adult neurones only 22% of the binding sites showed a high affinity for ifenprodil ($EC_{50} = 0{\cdot}013$ $\mu$M), whereas 78% of binding sites were of low affinity ($EC_{50} = 10{\cdot}5$ $\mu$M). Thus the fraction of

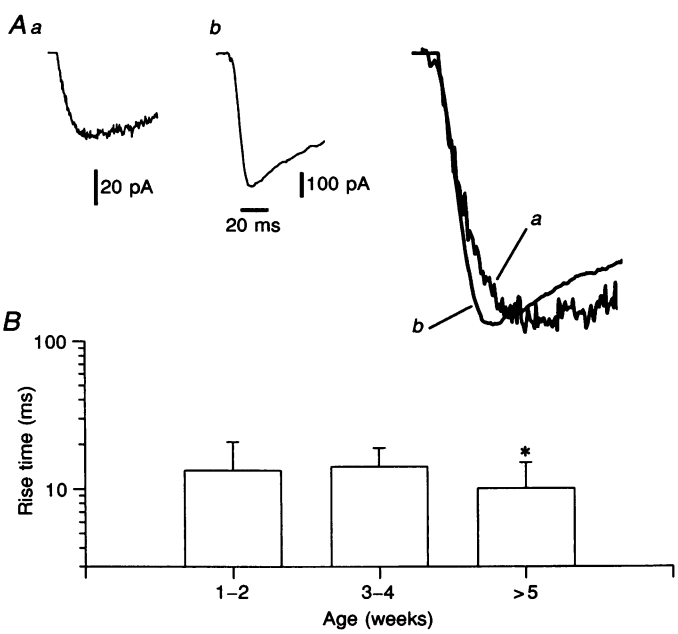


**Figure 6. The rise times of isolated NMDA EPSCs become faster with age**

Comparisons were made between NMDA EPSCs evoked in $Mg^{2+}$-free saline at −60 mV. *A*, representative traces of the rising phase of NMDA EPSCs in a 16-day-old (*A a*) and a 19-week-old PC (*A b*). Their respective rise times are 18·8 (*A a*) and 8 ms (*A b*). The same traces are normalized and superimposed on the right. *B*, mean EPSC rise times (means ± S.D.) from 1- to 2-week-old ($n = 39$), 3- to 4-week-old ($n = 26$) and >5-week-old PCs ($n = 53$). * represents a significant difference compared with both other age groups ($P < 0{\cdot}05$, Student's *t* test).

low affinity ifenprodil binding to synaptic NMDA receptors in adult PCs was significantly (1·4-fold) bigger than in young neurones ($P < 0·0001$).

In five young and eleven adult PCs we were able to test the affect of at least four different ifenprodil concentrations on the NMDA EPSC in a single neurone. Representative results are illustrated in Fig. 10. The NMDA EPSCs in the young PC (Fig. 10*A*) were smaller and clearly much more sensitive to ifenprodil than those in the adult PC (Fig. 10*B*). In each case the concentration–response relation fitted a two binding-site model. The $EC_{50}$ values for high and low affinity binding components in these two neurones were quite similar to the respective mean $EC_{50}$ values from all neurones (Fig. 9). These data strongly suggest that the high and low affinity binding sites for ifenprodil at synaptic NMDA receptors may be co-expressed in a single PC. It should be noted, however, that because of the limited number of points in these concentration–response curves, we could not in some cases prefer a two over a one binding-site model with a Hill coefficient less than unity.

### Effect of ifenprodil on NMDA-induced currents

Ifenprodil was shown to block certain types of $Ca^{2+}$ channels in cultured hippocampal PCs with an $EC_{50}$ of $17 \pm 3$ μM (Church, Fletcher, Baxter & MacDonald, 1994).

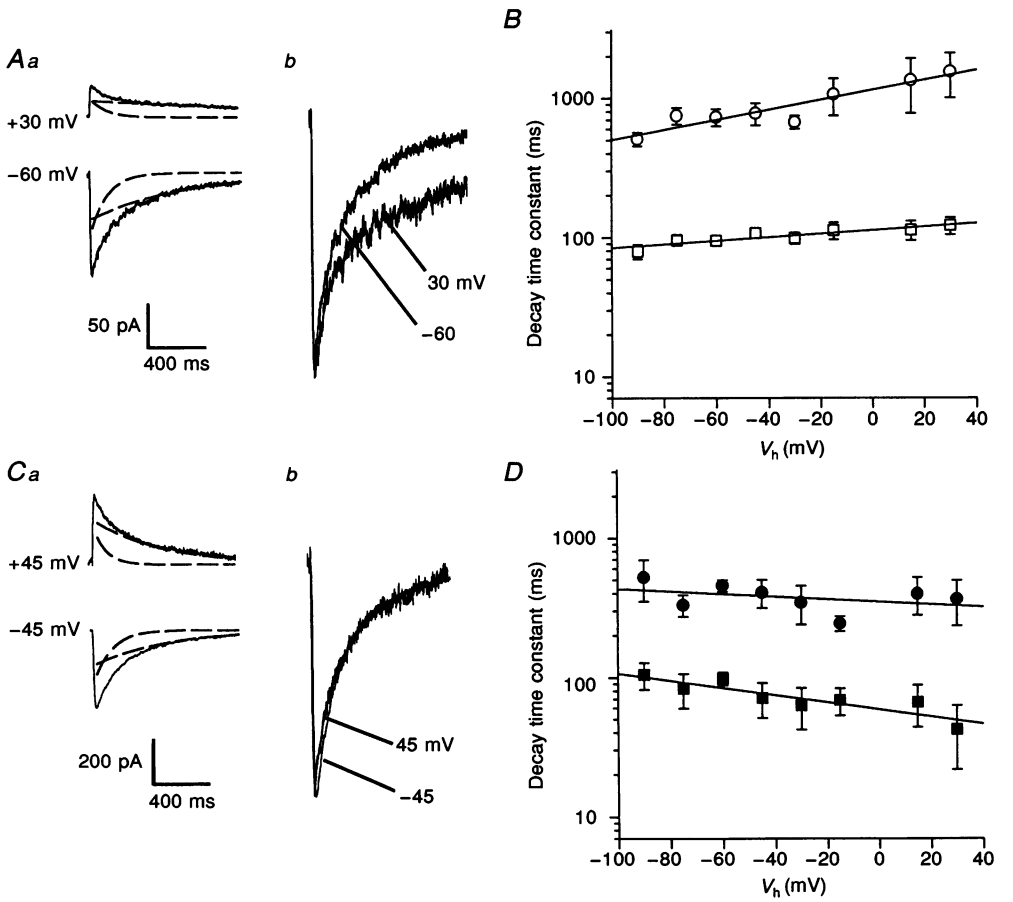


**Figure 7. Developmental switch in the voltage dependence of the decay time constants of NMDA EPSCs**

The EPSCs were evoked in $Mg^{2+}$-free saline at membrane potentials between −90 and +30 mV. Representative EPSCs from a young PC (5 days old) recorded at −60 and +30 mV (*A a*). The fast and slow decay components are superimposed on the EPSCs (dashed lines). The $\tau_f$ and $\tau_s$ values are 113·7 and 640·8 ms at −60 mV, and 108·9 and 1879 ms at +30 mV, respectively. The EPSCs scaled to the same peak amplitude are shown superimposed in *A b*. Note the slowing of decay time with depolarization. *B*, plots of $\tau_f$ (□) and $\tau_s$ (○) *versus* membrane potential in young mice (1–4 weeks old) (means ± S.E.M.; $n = 30$). Both decay time constants increased significantly with depolarization (Pearson linear correlation, $P < 0·05$, $r^2 = 0·81$ for $\tau_f$ and 0·85 for $\tau_s$). *Ca*, same as in *A* except that NMDA EPSCs are from an adult PC (19 weeks old). The $\tau_f$ and $\tau_s$ values are 121·7 and 493·3 ms at −45 mV, and 86·8 and 475·7 ms at +45 mV, respectively. note a slight decrease in initial decay time with depolarization (*C b*). *D*, same as in *B* with plots of $\tau_f$ (■) and $\tau_s$ (●) *versus* membrane potential but from adult mice (>5 weeks old) (mean ± S.E.M.; $n = 10$). Only $\tau_f$ (■) decreased significantly with depolarization (Pearson linear correlation, $P < 0·05$, $r^2 = 0·79$).

If a similar effect is exerted at excitatory presynaptic terminals ending on CA1 PCs, then ifenprodil may depress NMDA EPSCs irrespective of binding to postsynaptic NMDA receptors. In order to verify that native NMDA receptors contain both high and low affinity binding sites for this drug, we examined the affect of ifenprodil on NMDA receptor-mediated currents evoked by iontophoretic application of NMDA in tetrodotoxin-treated CA1 PCs.

As illustrated in Fig. 11, NMDA-induced currents were blocked by ifenprodil in a concentration-dependent manner in both young (Fig. 11*A*) and adult (Fig. 11*B*) neurones. The ifenprodil concentration–response relations (Fig. 11*C*) were accurately described by a two binding-site model, with 19% high ($EC_{50}$ of 0·059 $\mu$M) and 81% low affinity binding sites ($EC_{50}$ of 20·1 $\mu$M) in adult neurones ($n = 28$) and with 49% high ($EC_{50}$ of 0·036 $\mu$M) and 51% low affinity binding sites ($EC_{50}$ of 79·9 $\mu$M) in young neurones ($n = 28$). These relations were similar to those obtained for ifenprodil block of NMDA EPSCs (Fig. 9), though the $EC_{50}$ values were about 5-fold higher. Thus, these data indicate the presence of both high and low affinity ifenprodil binding to native NMDA receptors, but do not exclude the contribution of a presynaptic mechanism to the ifenprodil block of NMDA EPSCs.

This later point was further investigated by testing the affect of ifenprodil on pharmacologically isolated non-NMDA EPSCs and on currents induced by AMPA iontophoresis. As illustrated in Fig. 12*A*, ifenprodil blocked non-NMDA EPSCs only at high ifenprodil concentrations (>10 $\mu$M), without affecting AMPA-induced currents. The ifenprodil concentration–response relation for non-NMDA EPSCs was accurately described by a single binding-site model with an $EC_{50}$ of 38·5 $\mu$M and a Hill coefficient of 1·32 (Fig. 12*B*, ●). These data indicate that a presynaptic mechanism may contribute only to the low affinity block of NMDA EPSCs by ifenprodil.

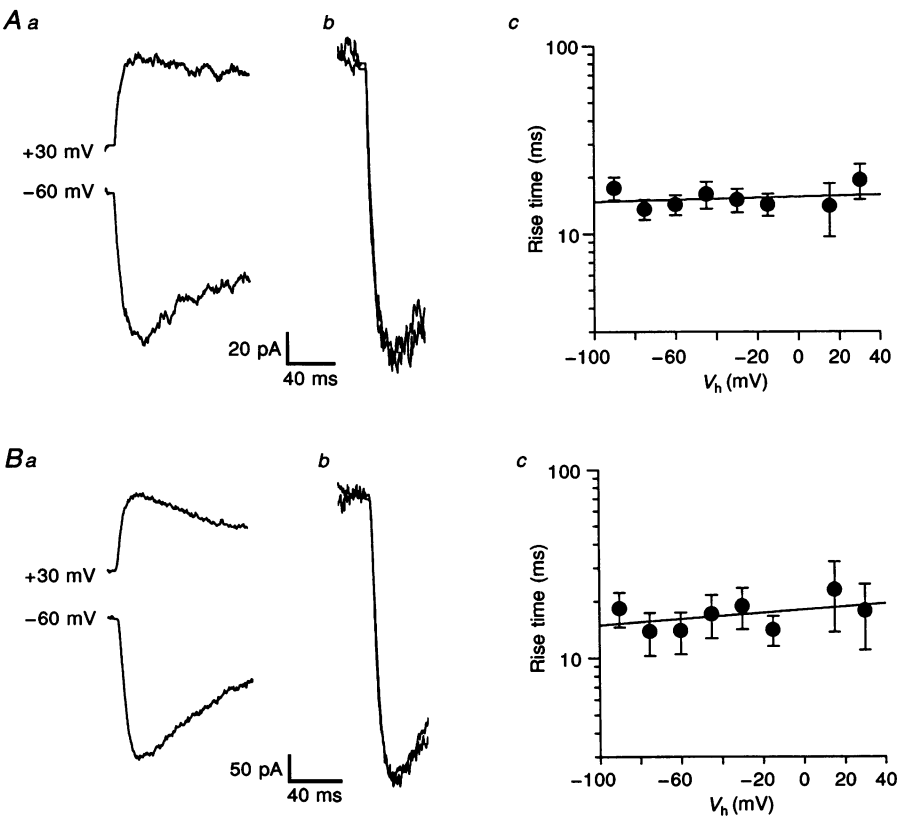


**Figure 8. The rise times of NMDA EPSCs are not voltage sensitive**

The EPSCs were evoked in $Mg^{2+}$-free saline at holding potentials between −90 and +30 mV. Exemplary traces of the rising phase of NMDA EPSCs from an 18-day-old PC recorded at −60 and +30 mV (*A a*). *A b*, the EPSCs scaled to the same peak amplitude are superimposed. The rise times at −60 mV (18 ms) and at +30 mV (15·4 ms) are similar. *A c*, plot of rise times *versus* membrane potential in 1- to 4-week-old PCs (means ± S.E.M.; $n = 17$). No significant correlation was found between the holding potential and rise times (Pearson linear correlation; $P > 0·05$). *B a*, same as in *A*, but from an 11-week-old PC. *B b*, the rise times at −60 mV (8·5 ms) and at +30 mV (10·5 ms) are similar. *B c*, plot of rise times *versus* membrane potential in >5-week-old PCs (means ± S.E.M.; $n = 8$). No significant correlation was found between holding potential and rise times (Pearson linear correlation; $P > 0·05$).

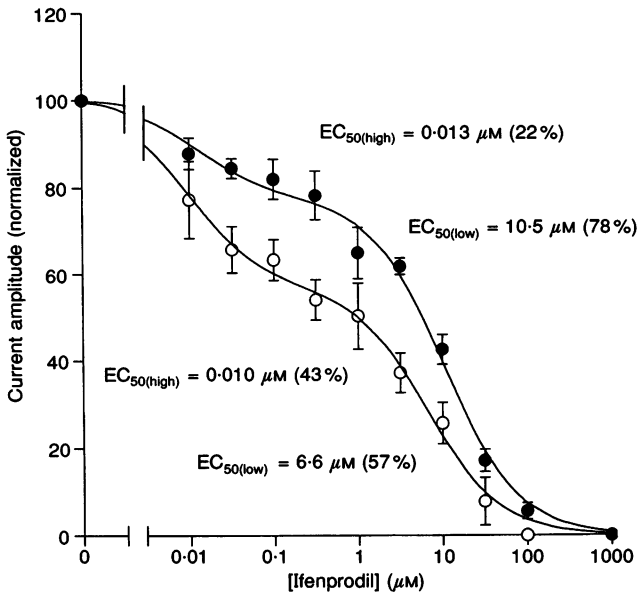


**Figure 9. Concentration–response curves for ifenprodil block of NMDA EPSCs in young *versus* adult PCs**

The NMDA EPSCs were evoked in $Mg^{2+}$-free saline at −60 mV. Mean concentration–response relations (means ± S.E.M.; $n$ = up to 16 for each concentration) are plotted for 1- to 4-week-old (○) and >5-week-old PCs (●). The results from each group were fitted with a two binding-site model (continuous line; see eqn (2) in Methods). The best fits were obtained with 43% high affinity and 57% low affinity binding sites for the young cells, *versus* 22% high affinity and 78% low affinity binding sites for the adult cells.

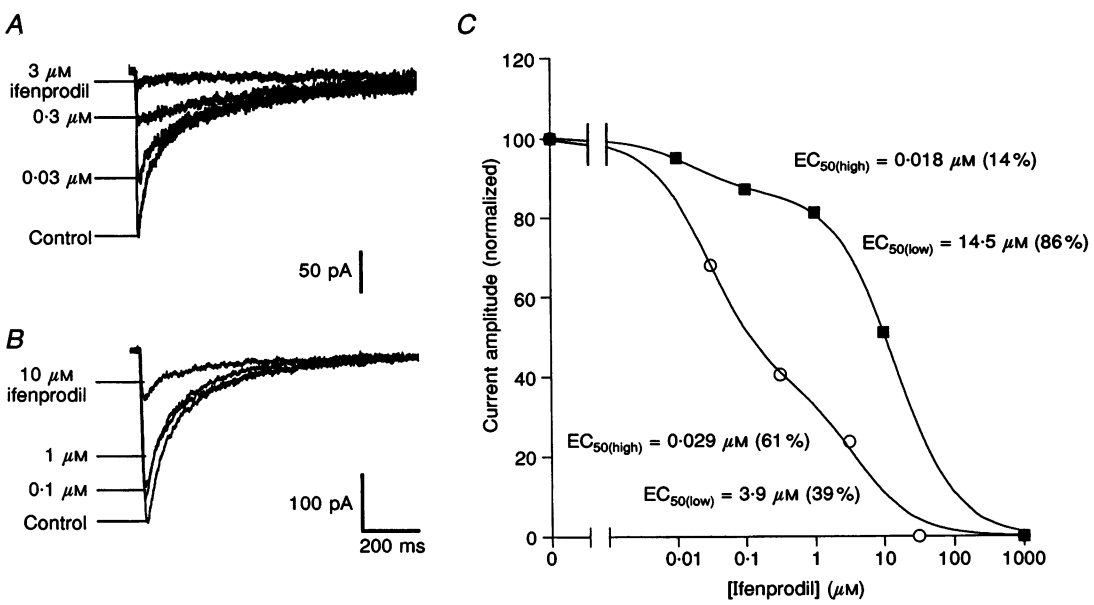


**Figure 10. Block of NMDA EPSCs by ifenprodil in single young *versus* adult PCs**

The EPSCs were evoked in $Mg^{2+}$-free saline at −60 mV. Superimposed records of EPSCs in control saline and in different ifenprodil concentrations from an 8-day-old PC (*A*) and from a 26-week-old PC (*B*). *C*, concentration–response relations of ifenprodil block in the cells illustrated in *A* (○) and in *B* (■). The data from each cell were fitted separately with a two binding-site model (continuous line; see eqn (2) in Methods). The best fits were obtained with 61% high affinity and 39% low affinity binding sites for the young cell, *versus* 14% high affinity and 86% low affinity binding sites for the adult cell.

### Effect of ifenprodil on NMDA EPSC decay

It is generally accepted that the slow NMDA EPSC decay is determined postsynaptically by the kinetics of the receptor channels (Hestrin, Sah & Nicoll, 1990), but the reason for the two decay components is not yet obvious. An attractive possibility is that each component reflects the decay kinetics of a distinct receptor subunit combination. To test whether the two decay components may differ pharmacologically, we determined their individual sensitivity to ifenprodil. In sixteen PCs (displaying both high and low affinity ifenprodil binding components), the differential concentration–response relations for ifenprodil block of $A_f$ and $A_s$ were not consistently different from each other. Furthermore, the ratio $A_f : A_s$ did not correlate directly or inversely with the ratio of the high and low affinity ifenprodil binding components ($r^2 = 0{\cdot}03$; Pearson linear correlation). Finally, 0·3 $\mu$M ifenprodil, which would be expected to completely saturate the high affinity ifenprodil binding sites (Figs 9 and 10), did not alter the NMDA EPSC decay time course ($n = 8$, $P > 0{\cdot}05$; Wilcoxon paired test) (Fig. 13*A*). Taken together, these data indicate that the NMDA components displaying fast *versus* slow decay kinetics are equally sensitive to ifenprodil.

We also tested whether the voltage sensitivity of EPSC duration in young PCs may be related to the large proportion of high affinity ifenprodil binding sites. At a concentration which is expected to saturate the high affinity binding sites (0·3 $\mu$M), ifenprodil had no effect on the voltage-dependent increase of NMDA EPSC decay (Fig. 13*B*; $n = 3$). This finding is inconsistent with an NMDA receptor subunit-dependent voltage sensitivity of NMDA EPSC decay.

## DISCUSSION

In this study we have characterized the developmental changes of several physiological and pharmacological properties of NMDA EPSCs in hippocampal CA1 PCs. We found that the main changes are expressed in the kinetics of these currents, rather than in their sensitivity to $Mg^{2+}$. These changes are paralleled by a decrease in the fraction of high affinity binding sites for the subunit-specific NMDA receptor antagonist ifenprodil. These findings cast light on the putative subunit composition of native synaptic NMDA receptors in young *versus* adult PCs and suggest that developmental changes in this composition may have important consequences for synaptic function and plasticity.

### Amplitude of NMDA EPSCs

The size and complexity of mouse CA1 PCs markedly increased in the first few postnatal weeks, as previously shown in the rat (Pokorny & Yamamoto, 1981). This was associated with a 4-fold increase in the size of neurally

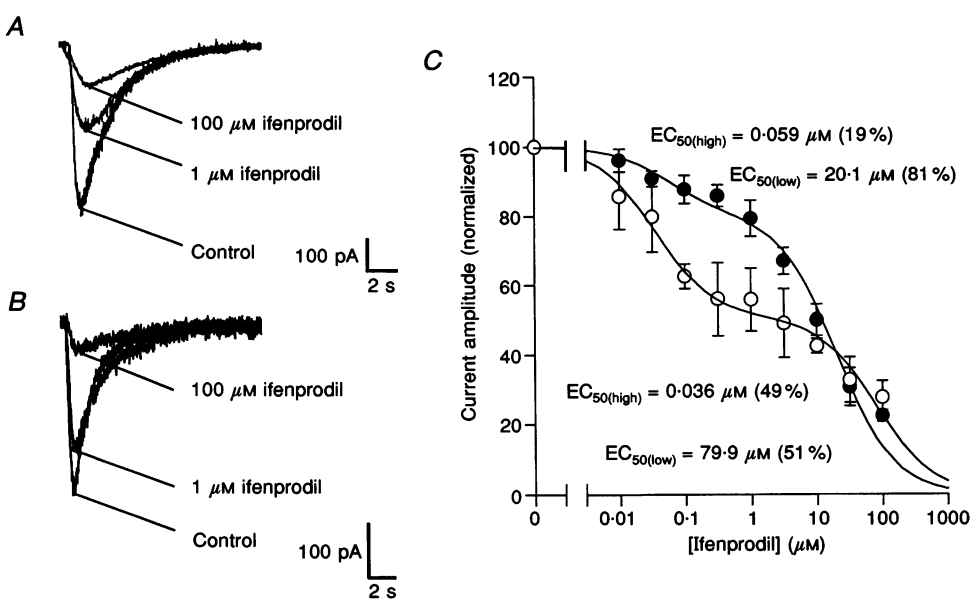


**Figure 11. Block of NMDA-induced currents by ifenprodil**

NMDA was applied by iontophoresis (< 1 s; < 1 $\mu$A) from a pipette containing 100 mM NMDA, positioned about 100 $\mu$M apical to the PC soma. The currents were evoked in $Mg^{2+}$-free saline at −60 mV. *A* and *B* are sample records depicting the control response and the effect of 1 and 100 $\mu$M ifenprodil in representative PCs from 9-day-old (*A*) and 20-week-old mice (*B*). *C*, normalized ifenprodil concentration–response curve in young (○) *versus* adult PCs (●) (means ± S.E.M.; $n$ = up to 8 for each concentration). The results were fitted with a two binding-site model (continuous line; see eqn (2) in Methods). The best fit was obtained with 49% high affinity ($EC_{50}$, 0·036 $\mu$M) and 51% low affinity ($EC_{50}$, 79·9 $\mu$M) binding sites in the young group, *versus* 19% high affinity ($EC_{50}$, 0·059 $\mu$M) and 81% low affinity ($EC_{50}$, 20·1 $\mu$M) binding sites in the adult.

evoked NMDA EPSCs. Recent studies of glutamatergic transmission in developing rat CA1 PCs have shown a steady increase in the size of the compound excitatory postsynaptic potentials between postnatal weeks 2–3 and 4–5 (Bekenstein & Lothman, 1991; Dumas & Foster, 1995). In the latter study this increase was shown to involve, at least in part, an increase in the probability of quantal transmitter release. In addition synaptic contacts on CA1 PCs continue to exhibit rapid growth until the fourth postnatal week (Steward & Falk, 1991). Thus development of presynaptic function associated with synapse formation may underlie the postnatal increase in NMDA EPSC size.

**Magnesium sensitivity**

Our data indicate that in mouse CA1 PCs, the sensitivity of synaptic NMDA receptors to extracellular $Mg^{2+}$ does not change after the first few postnatal days. The apparent $K_d$ values for $Mg^{2+}$ binding to synaptic NMDA receptors in very young, intermediate and adult neurones (7·8 ± 6·4, 10·4 ± 14·1 and 6·5 ± 4·7 mM, respectively, at 0 mV) were not significantly different from each other. In a recent study using single NMDA receptor-channel analysis (Strecker *et al.* 1994), the $K_d$ value for $Mg^{2+}$ binding to extrasynaptic NMDA receptors in 2-week-old rat CA1 PCs (6·8 mM, at 0 mV) was very similar to those reported here. The $K_d$ for $Mg^{2+}$ binding in neonates also was the same (4·9 mM at 0 mV; Strecker *et al.* 1994). Taken together, these data indicate that the affinity of NMDA receptors for $Mg^{2+}$ in rodent CA1 PCs may not change significantly after birth.

Our findings are at odds with two earlier studies of NMDA receptors in young *versus* adult rat CA1 PCs. In the first study (Bowe & Nadler, 1990) a grease-gap method was used to record NMDA-induced depolarizations in CA1. It was found that $Mg^{2+}$ antagonized the responses to NMDA in young (10- to 15-day-old) less potently than in adult slices, suggesting a developmental increase in the $Mg^{2+}$ sensitivity of NMDA receptors. However, a decrease in NMDA receptor density in adult neurones also would account for this finding (Bowe & Nadler, 1990). In the second study (Morrisett, Mott, Lewis, Wilson & Swartzwelder, 1990) neurally evoked NMDA receptor-mediated responses were recorded extracellularly in CA1 in picrotoxin-treated, thick (625 μm) slices. It was found that $Mg^{2+}$ (in the millimolar concentration range) was less effective in blocking the integrated extracellular responses in young (25- to 35-day-old) than in adult (75- to 90-day-old) preparations. Although this finding is consistent with a developmental increase in the $Mg^{2+}$ sensitivity of NMDA receptors, it is not the only possible conclusion. In adult, thick, picrotoxin-treated slices

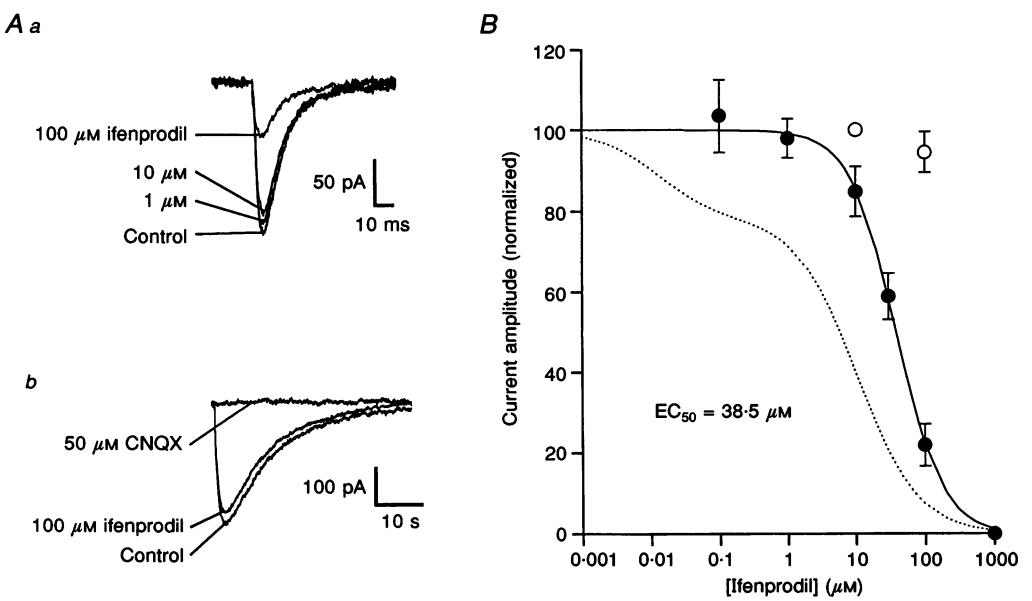


**Figure 12. Low affinity block of non-NMDA EPSCs by ifenprodil**

Non-NMDA EPSCs were evoked at −60 mV in the presence of 100 μM D-aminophosphonovalerate. Non-NMDA receptor-mediated currents were evoked by AMPA iontophoresis (500 ms; 200 nA) from a pipette containing 100 mM AMPA, positioned about 100 μM apical to the PC soma. *A a*, a sample of non-NMDA EPSCs depicting the control response and the effect of 1–100 μM ifenprodil in an adult PC. *A b*, a sample of iontophoretic AMPA-induced currents depicting the lack of effect of ifenprodil (100 μM) on this non-NMDA receptor type. The currents could be blocked completely by CNQX (50 μM). Note the different time scale of the iontophoretic responses. *B*, normalized ifenprodil concentration–response relations (means ± S.E.M.; $n = 4$–8 for each concentration) for non-NMDA EPSCs (●) *versus* iontophoretic AMPA-induced currents (○). The results for non-NMDA EPSCs were fitted with a one binding-site model (continuous line; see eqn (1) in Methods). The best fit was obtained with an $EC_{50}$ of 38·5 μM. The curve fitted to the concentration–response relation of adult NMDA EPSCs is plotted on the same graph (dotted line) for comparison.

a greater contribution of polysynaptic activity may render the NMDA receptor-mediated activity more sensitive to high concentrations of $Mg^{2+}$, even if the $Mg^{2+}$ sensitivity of NMDA receptors does not change.

It should be noted, however, that the data used for the young group was from neurones from postnatal day 4–14 mice. Changes in $Mg^{2+}$ sensitivity of NMDA receptors in the first few postnatal days might occur as suggested by Kleckner & Dingledine (1991; but see Strecker *et al.* 1994).

### NMDA EPSC time course

In agreement with previous descriptions in 2- to 3-week-old rat hippocampal neurones (Keller *et al.* 1991; Perouansky & Yaari, 1993), the decay time course of NMDA EPSCs in both young and adult mouse PCs consisted of a fast and a slow exponential component. Additionally, we found that during postnatal maturation both $\tau_f$ and $\tau_s$ decreased, though the relative contribution of each component ($A_f$ and $A_s$, respectively) to the NMDA EPSC did not change. Decrease in duration of NMDA EPSCs was previously observed in developing subcortical (Hestrin, 1992) and neocortical neurones (Carmignoto & Vicini, 1992). However, in the latter case the decrease was mostly due to reduction in $A_s$, with $\tau_s$ decreasing only mildly.

It is generally believed that the time course of neurally released L-glutamate in the synaptic cleft is very brief (up to 4 ms; Clements, Lester, Tong, Jahr & Westbrook, 1992), so that the slow time course of NMDA EPSCs reflects the slow kinetics of NMDA receptor channels (Hestrin *et al.* 1990; Lester, Clements, Westbrook & Jahr, 1990). Several lines of evidence suggest that the slow kinetics of these channels is determined primarily by the slow dissociation kinetics of L-glutamate (e.g. Lester & Jahr, 1993). Accordingly, the developmental decrease in NMDA EPSC duration suggests that the binding affinity of L-glutamate to synaptic NMDA receptors decreases in the first few weeks after birth.

### Voltage dependence of NMDA EPSC kinetics

As previously shown in young dentate granule cells (Konnerth *et al.* 1990) and superior colliculus neurones (Hestrin, 1992), the duration of NMDA EPSCs in young CA1 PCs was prolonged by depolarization. This was manifested as an increase in $\tau_f$ and $\tau_s$ upon depolarization without a significant change in $A_f$ and $A_s$. The mechanism underlying this voltage dependence is not known. Most probably it reflects an effect of voltage on channel kinetics, since the duration of NMDA receptor-mediated currents in excised outside-out patches from young superior colliculus neurones also increased with depolarization (Hestrin, 1992).

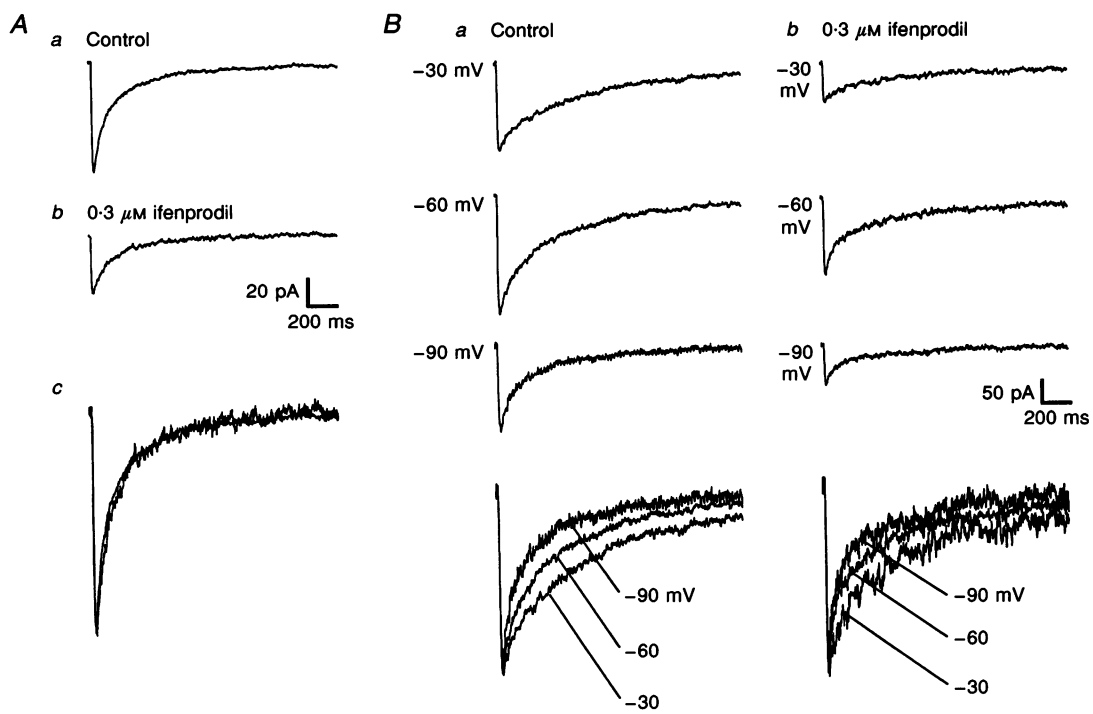


**Figure 13. Ifenprodil blocks NMDA EPSCs without affecting EPSC decay time course or voltage sensitivity**

*A*, EPSCs in an 8-day-old PC were evoked in $Mg^{2+}$-free saline at −60 mV in (*A a*) control saline ($\tau_f = 71$ ms; $\tau_s = 487$ ms) and (*A b*) after addition of 0·3 μM ifenprodil ($\tau_f = 70$ ms; $\tau_s = 490$ ms). *A a* and *A b* are scaled and superimposed for comparison (*A c*). No differences in decay time course were noted. *B*, NMDA EPSCs evoked at −30, −60 and −90 mV in $Mg^{2+}$-free saline in a 12-day-old PC. *Ba*, exemplary traces recorded at the indicated holding potentials are normalized and superimposed below. A lengthening of the decay phase with depolarization is evident. *Bb* same as *Ba* but after block by 0·3 μM ifenprodil. Note that the voltage dependence on the decay time remains unchanged.

Under the assumption that agonist unbinding kinetics determine the duration of NMDA EPSCs (Lester & Jahr, 1992), these findings would indicate that in young CA1 PCs depolarization increases the affinity of NMDA receptors for L-glutamate.

The voltage dependence of NMDA EPSC duration appeared to be developmentally regulated, as it was absent in adult CA1 PCs. In the latter neurones, however, the fast EPSC decay component was modestly accelerated by depolarization. This may be due to a direct effect of membrane potential on channel gating (rather than indirectly through an effect on agonist affinity). This effect may be present also in young CA1 PCs, though it would be masked by the more prominent effect of depolarization on NMDA receptor affinity for L-glutamate.

### High and low affinity ifenprodil inhibition

The concentration–response curves for ifenprodil block of NMDA EPSCs and iontophoretic NMDA-induced currents in CA1 PCs were biphasic, indicating the presence of high and low affinity ifenprodil binding sites at native NMDA receptors. A biphasic concentration–response curve was previously obtained in voltage-clamp recordings of NMDA-induced currents in *Xenopus* oocytes expressing NMDA receptors after injection of RNA from developing rat brains; the high and low affinity $EC_{50}$ values were 0·47 and 200 $\mu$M, respectively (Williams *et al.* 1993). Ifenprodil binding to NMDA receptors in cultured hippocampal neurones could also be separated into high ($EC_{50}$, 0·75 $\mu$M) and low affinity ($EC_{50}$, 161 $\mu$M) components (Legendre & Westbrook, 1991).

The $EC_{50}$ values for high and low affinity inhibition by ifenprodil were both about 5-fold lower for NMDA EPSCs (0·01 and 6·6 $\mu$M *versus* 0·01 and 10·5 $\mu$M in young *versus* adult neurones, respectively) than for NMDA-induced currents (0·06 and 20·1 $\mu$M *versus* 0·04 and 79·9 $\mu$M in young *versus* adult neurones, respectively). One possible explanation for this discrepancy is a block of L-glutamate release by ifenprodil acting on presynaptic $Ca^{2+}$ channels (Church *et al.* 1994), which would affect only NMDA EPSC inhibition. However, in view of the insensitivity of non-NMDA EPSCs to ifenprodil concentrations of up to 10 $\mu$M, such a mechanism may explain only the discrepancy in the low affinity $EC_{50}$ values. Alternatively, synaptic NMDA receptors may be more sensitive to ifenprodil than non-synaptic receptors activated by NMDA iontophoresis. In addition, the relatively prolonged exposure to high agonist concentrations during iontophoresis (0·1–1 s) is likely to cause NMDA receptors to undergo several forms of desensitization (e.g. Mayer, Vyklicky & Clements, 1989), which may render them less sensitive to ifenprodil. These explanations possibly account also for the differences between ifenprodil $EC_{50}$ values obtained in this study and those obtained previously using bath-applied NMDA (Legendre & Westbrook, 1991; Williams *et al.* 1993).

The high affinity component was significantly larger in young (43–49%) than in adult (22–20%) PCs, suggesting that NMDA receptors may undergo structural changes during postnatal development. These results agree with a recent study of NMDA receptors in whole rat brain membranes using ligand binding assays, which indicated the predominance of high affinity ($EC_{50}$, 0·65 $\mu$M) ifenprodil binding in the neonatal brain (Williams *et al.* 1993). During postnatal development the density of NMDA receptors increased by approximately 7-fold. Concomitantly, low affinity ($EC_{50}$, 76 $\mu$M) ifenprodil binding sites appeared, accounting for 50% of ifenprodil binding in the adult brain (Williams *et al.* 1993).

### Putative subunit composition of synaptic NMDA receptors in young *versus* adult PCs

The distinguishing properties of NMDA EPSCs in young and adult PCs described in this study and the corresponding features of L-glutamate-induced currents in host cells expressing one of the four recombinant heteromeric NMDA receptors (taken from Monyer *et al.* 1992; 1994), are summarized in Table 1. It can be seen that with respect to $Mg^{2+}$ binding (apparent $K_d$ at 0 mV), synaptic NMDA receptors in both very young (7·8 mM), intermediate (10·4 mM) and adult PCs (6·5 mM) are similar to NR1–NR2A (8·2 mM) and NR1–NR2B receptors (8·2 mM), and differ markedly from NR1–NR2C (18·9 mM) and NR1–NR2D receptors (36·3 mM). Likewise, $\tau_f$ (about 90 ms) of synaptic NMDA receptors in both young and adult PCs is closest to the offset decay time constant ($\tau_{off}$) of the NR1–NR2A receptors (118 ± 11 ms), whereas $\tau_s$ (500–800 ms) approximates the $\tau_{off}$ values of the NR1–NR2B (400 ± 49 ms) and NR1–NR2C (382 ± 45 ms) receptors. None of these values is similar to the $\tau_{off}$ value of NR1–NR2D receptors (4·8 ± 0·9 s).

The exact number and identity of NR2 subunits incorporated in native NMDA receptors is not yet known (Wafford *et al.* 1993). Under the simplest assumption that native synaptic NMDA receptors in CA1 PCs are NR1–NR2 heteromers, their relatively high affinity for $Mg^{2+}$ and fast decay kinetics suggest that they may comprise the NR1–NR2A and/or the NR1–NR2B assemblies. The existence of distinct high and low affinity binding sites for ifenprodil is consistent with this hypothesis. The developmental shift to faster decay kinetics and the concomitant decrease in high affinity ifenprodil binding sites suggests a developmental increase in the proportion of NR1–NR2A receptors. This conclusion is supported by recent studies utilizing *in situ* hybridization, showing that only the NR1, NR2A and NR2B subunits are expressed in hippocampal PCs (Moriyoshi *et al.* 1991; Kutsuwada *et al.* 1992), and that the expression of NR2A increases throughout postnatal development (Monyer *et al.* 1994; Mori & Mishina, 1995).

Biphasic concentration–response relations were observed at the single pyramidal cell level, suggesting that high and low ifenprodil binding sites may co-exist in the same neurone. We speculated whether these two binding sites, corresponding to the NR1–NR2B and NR1–NR2A subunit combinations

**Table 1. Functional properties of native synaptic NMDA receptors (A) *versus* four different recombinant heteromeric NMDA receptors (B)**

| A. | | Synaptic NMDA receptors | | | | | |
|---|---|---|---|---|---|---|---|
| | | 1–2 weeks old | *n* | 3–4 weeks old | *n* | >5 weeks old | *n* |
| EPSC amplitude (0 $Mg^{2+}$) (pA) | | 74·6 ± 47·4 | 42 | 127·6 ± 101·6 | 27 | 262·7 ± 158·5 | 56 |
| EPSC amplitude (1 mM $Mg^{2+}$) (pA) | | 12·1 ± 5·6 | 4 | 17·9 ± 7·2 | 7 | 45·9 ± 17·3 | 8 |
| $Mg^{2+}$ block at −60 mV (%) | | 88·2 ± 2·1 | 4 | 84·2 ± 5·8 | 7 | 81·1 ± 10·1 | 8 |
| $V_h$ of maximal inward NMDA current in 1 mM $Mg^{2+}$ (mV) | | −30 | | −30 | | −30 | |
| Apparent $K_d$ of $Mg^{2+}$ binding at 0 mV (mM) | | 7·8 ± 6·4 | 14 | 10·4 ± 14·1 | 14 | 6·5 ± 4·7 | 12 |
| Deactivation kinetics (ms) | $\tau_f$ | 96 ± 37 | 43 | 96 ± 40 | 26 | 84 ± 42 | 52 |
| | $\tau_s$ | 861 ± 545 | 43 | 707 ± 452 | 26 | 494 ± 359 | 52 |
| Contribution of $A_f$ (%) | | 61·3 ± 16 | 43 | 56·2 ± 15 | 26 | 60·2 ± 15 | 52 |
| Rise time (ms) | | 13·3 ± 8 | 39 | 14·2 ± 5 | 26 | 10·1 ± 5 | 53 |

| | | Synaptic NMDA receptors | | | |
|---|---|---|---|---|---|
| | | 1–4 weeks old | *n* | >5 weeks old | *n* |
| e-fold increase of EPSC decay (mV) | $\tau_f$ | +343 | | −167 | |
| | $\tau_s$ | +121 | | — | |
| $EC_{50}$ of ifenprodil block (μM) | high affinity | 0·010 | 23 | 0·013 | 30 |
| | low affinity | 6·6 | 23 | 10·5 | 30 |

| B. | Recombinant NMDA receptors | | | |
|---|---|---|---|---|
| | NR1–NR2A | NR1–NR2B | NR1–NR2C | NR1–NR2D |
| EPSC amplitude (0 $Mg^{2+}$) (pA) | — | — | — | — |
| EPSC amplitude (1 mM $Mg^{2+}$) (pA) | — | — | — | — |
| $Mg^{2+}$ block at −60 mV (%) | n.d. | n.d. | n.d. | n.d. |
| $V_h$ of maximal inward NMDA current in 1 mM $Mg^{2+}$ (mV) | −25* | −25* | −45* | −45* |
| Apparent $K_d$ of $Mg^{2+}$ binding at 0 mV (mM) | 8·2 | 8·2 | 18·9 | 36·3 |
| Deactivation kinetics (ms) $\tau_f$ | 118 ± 11‡ | 400 ± 49‡ | 382 ± 45‡ | 4·5 ± 0·9‡§ |
| $\tau_s$ | — | — | — | — |
| Contribution of $A_f$ (%) | — | — | — | — |
| Rise time (ms) | n.d. | n.d. | n.d. | n.d. |
| e-fold increase of EPSC decay (mV) | n.d. | n.d. | n.d. | n.d. |
| $EC_{50}$ of ifenprodil block (μM) | 146† | 0·34† | n.d. | n.d. |

* From Monyer *et al.* 1994; † from Williams, 1993; ‡ means ± S.E.M.; § results in seconds; n.d., not determined.

may account for the slow and fast exponential decay components of NMDA EPSCs, respectively. This hypothesis predicts that the ratio $A_f : A_s$ would increase during development in conjunction with the presumed increase in the proportion of NR1–NR2A receptors, and that ifenprodil would preferentially block $A_s$. However, the ratio $A_f : A_s$ did not change during development and ifenprodil reduced both $A_f$ and $A_s$ to the same extent, refuting this hypothesis.

## Physiological implications

Accumulating evidence suggests that NMDA receptor-mediated neuronal responses (Tsumoto *et al.* 1987), NMDA-dependent long-term potentiation of excitatory synaptic transmission (Harris & Teyler, 1984) and NMDA-induced neurotoxicity (McDonald, Silverstein & Johnston, 1988) are markedly enhanced in the developing brain. One reason for this enhancement could be the late postnatal maturation of GABAergic inhibition (Zhang, Spigelman & Carlen, 1991), which in the adult brain normally prevents the sustained activation of NMDA receptors (Dingledine, Hynes & King, 1986). An alternative or complementary reason could be increased efficacy of the NMDA receptors themselves. It was suggested previously that $Mg^{2+}$ antagonizes the depolarizing action of NMDA less potently in hippocampal neurones of young rather than of adult rats (Bowe & Nadler, 1990; Morrisett *et al.* 1990). Though we and others (Strecker *et al.* 1994) could not confirm this particular notion, our data suggest that the affinity of L-glutamate to the NMDA

receptors is higher in young than in adult CA1 PCs, resulting in more prolonged NMDA EPSCs. Furthermore, depolarization of young neurones, presumably by strengthening the binding of the transmitter to the NMDA receptor, further prolongs the duration of the EPSCs. Consequently, NMDA EPSCs would be more effective in young rather than adult PCs in conveying the electrical and $Ca^{2+}$ signals required for neuronal plasticity.


ARMSTRONG-JAMES, M., WELKER, E. & CALLAHAN, C. A. (1993). The contribution of NMDA and non-NMDA receptors to fast and slow transmission of sensory information in the rat SI barrel cortex. *Journal of Neuroscience* **13**, 2149–2160.

ASCHER P. & NOWAK L. (1988). The role of divalent cations in the *N*-methyl-D-aspartate responses of mouse central neurons in culture. *Journal of Physiology* **399**, 247–266.

BEKENSTEIN, J. W. & LOTHMAN, E. W. (1991). A comparison of the ontogeny of excitatory and inhibitory neurotransmission in the CA1 region and dentate gyrus of the rat hippocampal formation. *Developmental Brain Research* **63**, 237–243.

BLISS, T. V. P. & COLLINGRIDGE, G. L. (1993). A synaptic model of memory: long-term potentiation in the hippocampus. *Nature* **361**, 31–39.

BOWE, M. A. & NADLER, J. V. (1990). Developmental increase in the sensitivity to magnesium of NMDA receptors on CA1 hippocampal pyramidal cells. *Developmental Brain Research* **56**, 55–61.

CARMIGNOTO, G. & VICINI, S. (1992). Activity-dependent decrease in NMDA receptor responses during development of the visual cortex. *Science* **258**, 1007–1011.

CHURCH, J., FLETCHER, E. J., BAXTER, K. & MACDONALD, J. F. (1994). Blockade by ifenprodil of high voltage-activated $Ca^{2+}$ channels in rat and mouse cultured hippocampal pyramidal neurons: comparison with *N*-methyl-D-aspartate receptor antagonist actions. *British Journal of Pharmacology* **113**, 499–507.

CLEMENTS, J. D., LESTER, R. A., TONG, G., JAHR, C. E. & WESTBROOK, G. L. (1992). The time course of glutamate in the synaptic cleft. *Science* **258**, 1498–1501.

DIEMER, N. H., VALENTE, E., BRUHN, T., BERG, M., JORGENSEN, M. B. & JOHANSEN, F. F. (1993). Glutamate receptor transmission and ischemic nerve cell damage: evidence for involvement of excitotoxic mechanisms. *Progress in Brain Research* **96**, 105–122.

DINGLEDINE, R., HYNES, M. A. & KING, G. L. (1986). Involvement of *N*-methyl-D-aspartate receptors in epileptiform bursting in the rat hippocampal slice. *Journal of Physiology* **380**, 175–189.

DUMAS, T. C. & FOSTER, T. C. (1995). Developmental increase in CA3–CA1 presynaptic function in the hippocampal slice. *Journal of Neurophysiology* **73**, 1821–1828.

EDWARDS, F. A., KONNERTH, A., SAKMANN, B. & TAKAHASHI, T. (1989). A thin slice preparation for patch clamp recordings from neurons of the mammalian central nervous system. *Pflügers Archiv* **414**, 600–612.

HARRIS, K. M., TEYLER, T. J. (1984). Developmental onset of long-term potentiation in area CA1 of the rat hippocampus. *Journal of Physiology* **346**, 27–48.

HESTRIN, S. (1992). Developmental regulation of NMDA receptor-mediated synaptic currents at a central synapse. *Nature* **357**, 686–689.

HESTRIN, S., SAH, P. & NICOLL, R. A. (1990). Mechanisms generating the time course of dual component excitatory synaptic currents recorded in hippocampal slices. *Neuron* **5**, 247–253.

KELLER, B. U., KONNERTH, A. & YAARI, Y. (1991). Patch clamp analysis of excitatory synaptic currents in granule cells of rat hippocampus. *Journal of Physiology* **435**, 275–293.

KLECKNER, N. W. & DINGLEDINE, R. (1991). Regulation of hippocampal NMDA receptors by magnesium and glycine during development. *Molecular Brain Research* **11**, 151–159.

KONNERTH, A., KELLER, B. U., BALLANYI, K. & YAARI, Y. (1990). Voltage sensitivity of NMDA-receptor mediated postsynaptic currents. *Experimental Brain Research* **81**, 209–212.

KUTSUWADA, T., KASHIWABUCHI, N., MORI, H., SAKIMURA, K., KUSHIYA, E., ARAKI, K., MEGURO, H., MASAKI, H., KUMANISHI, T., ARAKAWA, M. & MISHINA, M. (1992). Molecular diversity of the NMDA receptor channel. *Nature* **358**, 36–41.

LEGENDRE, P. & WESTBROOK, G. L. (1991). Ifenprodil blocks *N*-methyl-D-aspartate receptors by a two-component mechanism. *Molecular Pharmacology* **40**, 289–298.

LESTER, R. A. J., CLEMENTS, J. D., WESTBROOK, G. L. & JAHR, C. E. (1990). Channel kinetics determine the time course of NMDA receptor-mediated synaptic currents. *Nature* **346**, 565–567.

LESTER, R. A. J. & JAHR, C. E. (1993). NMDA channel behavior depends on agonist affinity, *Journal of Neuroscience* **12**, 635–643.

MCDONALD, J. W., SILVERSTEIN, F. S. & JOHNSTON, M. V. (1988). Neurotoxicity of *N*-methyl-D-aspartate is markedly enhanced in developing rat central nervous system. *Brain Research* **459**, 200–203.

MAYER, M. L., VYKLICKY, L. JR & CLEMENTS, J. (1989). Regulation of NMDA receptor desensitization in mouse hippocampal neurons by glycine. *Nature* **338**, 425–427.

MONYER, H., BURNASHEV, N., LAURIE, D. J., SAKMANN, B. & SEEBURG, P. H. (1994). Developmental and regional expression in the rat brain and functional properties of four NMDA receptors. *Neuron* **12**, 529–540.

MONYER, H., SPRENGEL, R., SCHOEPFER, R., HERB, A., HIGUCHI, M., LOMELI, H., BURNASHEV, N., SAKMANN, B. & SEEBURG, P. H. (1992). Heteromeric NMDA receptors: molecular and functional distinction of subtypes. *Science* **256**, 1217–1221.

MORI, H. & MISHINA, M. (1995). Structure and function of the NMDA receptor channel. *Neuropharmacology* **34**, 1219–1237.

MORIYOSHI, K., MASAYUKI, M., TAKAHIRO, I., RYUICHI, S., MIZUNO, N. & NAKANISHI, S. (1991). Molecular cloning and characterization of the rat NMDA receptor. *Nature* **354**, 31–37.

MORRISETT, R. A., MOTT, D. D., LEWIS, D. V., WILSON, W. A. & SWARTZWELDER, H. S. (1990). Reduced sensitivity of the *N*-methyl-D-aspartate component of synaptic transmission to magnesium in hippocampal slices from immature rats. *Developmental Brain Research* **65**, 257–262.

NOWAK, L., BREGESTOVSKI, P., ASCHER, P., HERBERT, A. & PROCHIANTZ, A. (1984). Magnesium gates glutamate activated channels in mouse central neurons. *Nature* **307**, 462–465.

PEARCE, R. A. (1993). Physiological evidence for two distinct $GABA_A$ responses in rat hippocampus. *Neuron* **10**, 189–200.

PEROUANSKY, M., BARANOV, D., SALMAN, M. & YAARI, Y. (1995). Effects of halothane on glutamate receptor-mediated excitatory postsynaptic currents: A patch-clamp study in adult mouse hippocampal slices. *Anesthesiology* **83**, 109–119.

PEROUANSKY, M. & YAARI, Y. (1993). Kinetic properties of NMDA receptor-mediated synaptic currents in rat hippocampal pyramidal cells *versus* interneurones. *Journal of Physiology* **465**, 223–244.

PORKONY, J. & YAMAMOTO, T. (1981). Postnatal ontogenesis of hippocampal CA1 area in rats. I. Development of dendritic arborization in pyramidal neurons. *Brain Research Bulletin* **7**, 113–120.

SAH, P., HESTRIN, S. & NICOLL, R. A. (1990). Properties of excitatory postsynaptic currents recorded *in vitro* from rat hippocampal interneurones. *Journal of Physiology* **430**, 605–616.

SPRUSTON, N., JAFFE, D. B., WILLIAMS, S. H. & JOHNSTON, D. (1993). Voltage- and space-clamp errors associated with the measurement of electrotonically remote synaptic events. *Journal of Neurophysiology* **70**, 781–802.

STEWARD, O. & FALK, P. M. (1991). Selective localization of polyribosomes beneath developing synapses: a quantitative analysis of the relationship between polyribosomes and developing synapses in the hippocampus and the dentate gyrus. *Journal of Comparative Neurology* **314**, 545–557.

STRECKER, G. J., JACKSON, M. B. & DUDEK, F. E. (1994). Blockade of NMDA-activated channels by magnesium in the immature rat hippocampus. *Journal of Neurophysiology* **72**, 1538–1548.

TSUMOTO, T., HAGIHARA, K., SATO, H. & HATA, Y. (1987). NMDA receptors in the visual cortex of young kittens are more effective than those of adult cats. *Nature* **327**, 513–514.

WAFFORD, K. A., BAIN, C. J., LE BOURDELLES, B., WHITING, P. J. & KEMP, J. A. (1993). Preferential co-assembly of recombinant NMDA receptors composed of three different subunits. *Molecular Neuroscience* **4**, 1347–1349.

WILLIAMS, K. (1993). Ifenprodil discriminates subtypes of the *N*-methyl-D-aspartate receptor: selectivity and mechanism at recombinant heteromeric receptors. *Molecular Pharmacology* **44**, 851–859.

WILLIAMS, K. (1995). Pharmacological properties of recombinant *N*-methyl-D-aspartate (NMDA) receptors containing the $\epsilon 4$ (NR2D) subunit. *Neuroscience Letters* **184**, 181–184.

WILLIAMS, K., RUSSELL, S. L., SHEN, Y. M. & MOLINOFF, P. B. (1993). Developmental switch in the expression of NMDA receptors occurs *in vivo* and *in vitro*. *Neuron* **10**, 267–278.

ZHANG, L., SPIGELMAN, I. & CARLEN, P. L. (1991). Development of GABA-mediated, chloride-dependent inhibition in CA1 pyramidal neurones of immature rat hippocampal slices. *Journal of Physiology* **444**, 25–49.

**Acknowledgements**

We thank Drs M. Perouansky and M. Jensen for their valuable comments, Mr G. Alroy for helping with the staining procedure and Ms H. Aharon for excellent technical assistance. The work was supported by the Israeli Ministry of Science and Technology and the German Israeli Foundation for Scientific Research and Development (GIF). E.D.K is a Foulkes fellow. This paper is dedicated to the memory of Dr Yoav Citri for his creativity, foresight and inspiration.

**Author's email address**

Y. Yaari: yaari@cc.huji.ac.il

*Received 15 April 1996; accepted 9 September 1996.*